Medicinal Chemistry

Deutsche Ausgabe: DOI: 10.1002/ange.201600868
Internationale Ausgabe: DOI: 10.1002/anie.201600868

Self-Assembly of Multi-nanozymes to Mimic an Intracellular Antioxidant Defense System

Yanyan Huang, Zhen Liu, Chaoqun Liu, Enguo Ju, Yan Zhang, Jinsong Ren,* and Xiaogang Qu**

Abstract: *In this work, for the first time, we constructed a novel multi-nanozymes cooperative platform to mimic intracellular antioxidant enzyme-based defense system. V_2O_5 nanowire served as a glutathione peroxidase (GPx) mimic while MnO_2 nanoparticle was used to mimic superoxide dismutase (SOD) and catalase (CAT). Dopamine was used as a linker to achieve the assembling of the nanomaterials. The obtained V_2O_5@pDA@MnO_2 nanocomposite could serve as one multi-nanozyme model to mimic intracellular antioxidant enzyme-based defense procedure in which, for example SOD, CAT, and GPx co-participate. In addition, through assembling with dopamine, the hybrid nanocomposites provided synergistic antioxidative effect. Importantly, both in vitro and in vivo experiments demonstrated that our biocompatible system exhibited excellent intracellular reactive oxygen species (ROS) removal ability to protect cell components against oxidative stress, showing its potential application in inflammation therapy.*

In biological organisms, reactive oxygen species (ROS), such as H_2O_2, $^{\bullet}OH$, and $O_2^{\bullet-}$, are continuously generated as byproducts of the metabolism of oxygen.[1] Appropriate ROS can serve as critical second messengers in cell signaling, pathogen defense, and homeostasis.[2] However, a high ROS level will exhibit detrimental influences on cells by causing lipid peroxidation, protein denaturation, or DNA damage.[3] These adverse reactions may lead to numerous human diseases such as inflammations and cancers.[4] To maintain the intracellular redox balance and protect the body against oxidative damage, enzymes such as catalase (CAT), superoxide dismutase (SOD), and glutathione peroxidase (GPx), work together to construct the intracellular antioxidant enzyme-based defense system.[5]

Due to the essential roles in cellular system, a growing research interest has been focused on the construction of artificial enzyme complex to mimic intracellular antioxidant enzyme-based defense process.[6] For example, Mugesh's group demonstrated that organic molecule isoselenazole could serve as both glutathione peroxidase and peroxiredoxin mimic to protect cells against oxidative damage.[6a] Recently, by assembling the catalytic centers of GPx and SOD on protein and polymer templates, respectively, Liu's group successfully designed two-enzyme-based antioxidative system.[6b] Though promising, the extraction of catalytic centers and the subsequent assembling on corresponding templates often needed complex genetic engineering with sophisticated instruments. Especially, these two enzyme-based antioxidative systems were limited in mimicking natural antioxidant defense system as in natural environment, multi-antioxidant enzymes (more than three enzymes), such as SOD, CAT and GPx, work together to co-construct the antioxidant enzyme-based defense system. To this end, it is highly desired to construct a simple and novel platform to mimic the complicated intracellular enzyme-based defense system.

With the development of nanotechnology, numerous functional nanomaterials are constantly emerging. Among them, nanozymes, as promising alternatives to natural enzymes, have attracted lots of research interests.[7] During the past decade, a series of nanozymes with unique antioxidant enzyme-like properties have been discovered.[8] For example, Pt, CeO_2, and MnO_2 nanomaterials have been discovered to possess CAT and SOD mimic activities which can remove harmful ROS.[8a–c] In addition, Mugesh et al. demonstrated that V_2O_5 nanowires exhibited remarkable GPx-like antioxidant property to protect cell against oxidative damage.[8d] All these findings provide a chance for the design of multi-antioxidative nanozyme complex to mimic cellular antioxidant enzyme system.

Inspired by these unique properties, herein, for the first time, we constructed a powerful multienzyme-cooperative platform to mimic intracellular antioxidant enzyme-based defense system. In our approach, V_2O_5 nanowire served as a GPx mimic while MnO_2 nanoparticle was used to mimic SOD and CAT. To assemble V_2O_5 nanowires with MnO_2 nanoparticles (Figure 1 A), dopamine was used to combine two nanomaterials together. In this way, the obtained V_2O_5@pDA@MnO_2 nanocomposites could serve as a multi-nanozyme model to mimic intracellular enzyme-based antioxidative process. Due to the unique SOD-like activity, MnO_2 nanomaterial could catalyze $O_2^{\bullet-}$ to generate O_2 and H_2O_2. The generated H_2O_2 could be further transformed to H_2O by MnO_2 nanomaterial with its' CAT-like property. Furthermore, with the intrinsic GPx-mimic capacity, V_2O_5 component could efficiently catalyze H_2O_2 to produce harmless products (Figure 1 B). This multi-antioxidation process could mimic

[*] Y. Huang, Z. Liu, C. Liu, E. Ju, Y. Zhang, Prof. J. Ren, Prof. X. Qu
Laboratory of Chemical Biology and
State Key Laboratory of Rare Earth Resource Utilization
Changchun Institute of Applied Chemistry
Chinese Academy of Sciences
Changchun, Jilin, 130022 (P.R. China)
E-mail: jren@ciac.ac.cn
xqu@ciac.ac.cn
Y. Huang, C. Liu, E. Ju, Y. Zhang
University of Chinese Academy of Sciences
Beijing 100039 (P.R. China)

Supporting information for this article can be found under: http://dx.doi.org/10.1002/anie.201600868.

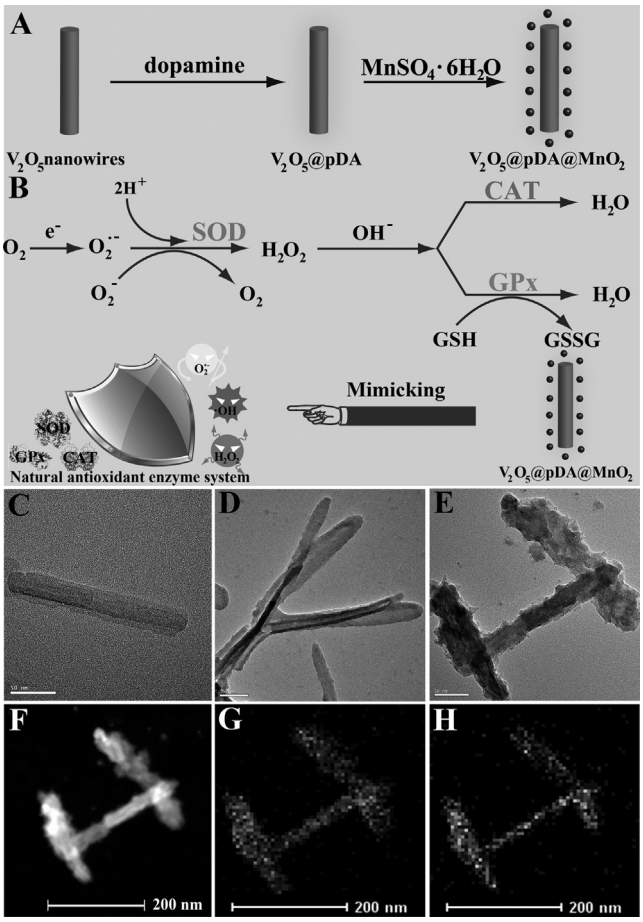

Figure 1. A) Scheme illustration of the synthesis of V_2O_5@pDA@MnO_2 nanocomposites. B) The reactive oxygen species removal progress of SOD-CAT-GPx synergetic system and the Scheme of our multi-nanozymes system to mimic intracellular antioxidant enzyme-based defense system; TEM images of V_2O_5 (C), V_2O_5@pDA (D) and V_2O_5@pDA@MnO_2 hybrid nanocomplex (E). Dark-field TEM image (F), and corresponding TEM elemental mappings of the V K-edge (G) and Mn K-edge signals (H).

intracellular antioxidant defense procedure in which SOD, CAT, GPx, etc. co-participated (Figure 1 B). In addition to the antioxidative activities of nanozymes, by assembling with dopamine, the nanocomposites provided synergistic antioxidative effect since dopamine could serve as an efficient antioxidant. Importantly, in vitro experiments demonstrated that our nanocomposites exhibited excellent intracellular ROS removal ability and could protect cell components against oxidative stress. Furthermore, an inflammation model was constructed to explore the potential application. With the assistance of nanocomposites, the ROS level in ear inflammation of mouse model decreased gradually, indicating the possibility of our nanocomposites in inflammation therapy. Taken together, our nanocomposites possessed multi-antioxidant enzyme-like properties which could mimic natural antioxidant enzyme-based defense system to protect the body against oxidative stress. Our new finding may pave the way for understanding the reaction mechanism of intracellular antioxidant enzyme-based defense system and promote the development of nanozyme-based cooperative system to mimic the natural antioxidative process.

To verify our hypothesis, V_2O_5 nanowires were first synthesized.[9] Subsequently, through the self-polymerization of dopamine, a uniform polydopamine (pDA) film was assembled on the surface of nanowires[10] (noted as V_2O_5@pDA). With the abundant functional groups, the formation of the pDA layer was contributed to the further synthesis of composite material.[11] In this way, MnO_2 nanoparticles were formed on the pDA layer[12] and the resultant product V_2O_5@pDA@MnO_2 nanocomposites (NCs) was obtained. The morphologies and compositions of these nanomaterials were fully characterized and the characterizations of V_2O_5 nanowires were carried out firstly. Figure S1 in the Supporting Information and Figure 1 C were the corresponding scanning electron microscopy (SEM) and transmission electron microscopy (TEM) images. SEM image indicated V_2O_5 nanowires were well dispersed with an average size of about 300 nm (Figure S2). The X-ray diffraction (XRD) pattern of the obtained powder was shown in Figure S3. After adding dopamine, a distinctly rougher surface was observed, illustrating the successfully assembly of pDA (Figure 1 D). Thermogravimetric analysis (TGA) data demonstrated about 60 % weight loss up till 800 °C (Figure S4). After reflux, small MnO_2 nanoparticles were assembled on the pDA layer (Figure 1 E and Figure S5) and V_2O_5@pDA@MnO_2 nanocomposites were formed. Figure 1 F–H was the dark-field TEM image and elemental mapping images of the nanocomposites. Uniform distribution of V and Mn were displayed in the system, illustrating the presence of V_2O_5 and MnO_2 components. The energy dispersive X-ray spectroscopy (EDX), X-ray photon spectroscopy (XPS) and XRD analysis (Figures S6, S7 and S8) further verified the successful assembly of nanocomposites. Fourier transform infrared spectroscopy spectra (Figure S9) and UV/Vis absorption spectroscopy (Figure S10) were also confirmed our design. Taken together, all results proved the assembly of V_2O_5@pDA@MnO_2 nanocomposites.

Having successfully fabricating the V_2O_5@pDA@MnO_2 nanocomposites, we then investigate their properties. The GPx-like activity was evaluated firstly. In the presence of GSH, V_2O_5 component could catalyze H_2O_2 to form harmless products (Figure S11).[8d] The generated GSSG could be returned to GSH with glutathione reductase (GR) and coenzyme NADPH. Therefore, by measuring the absorption of NADPH at 340 nm,[13] real-time monitoring of the reaction progress could be achieved. In Figure 2 A, an obvious decrease of NADPH concentration was observed only with all components present. We also compared the catalytic activities of different components (Figure S12). Although the GPx activity of V_2O_5 was compromised upon functionalization with pDA and subsequent incorporation of MnO_2, our nanocomposite still exhibited high catalytic activity. We then investigated the influence of catalyst and substrate concentrations on the biocatalytic property of nanocomposites. Upon increasing the concentration of nanocomposites, the absorption intensity decreased dramatically (Figure S13 A). In Figure 2 B and S13 B, the reaction rate increased with the increase of GSH and H_2O_2 concentration, respectively. The

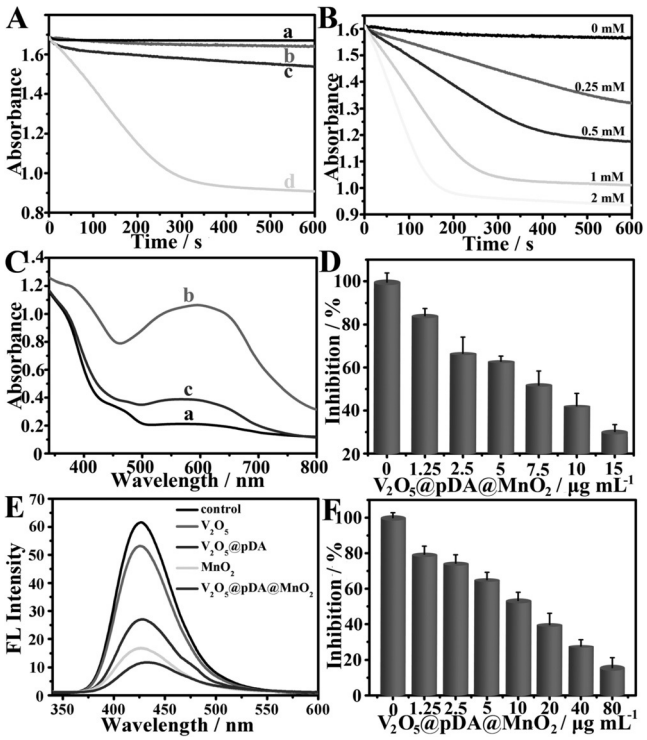

Figure 2. Antioxidant enzyme-like properties of nanocomposites: A) The study of GPx-like activity: a) without nanocomposites, b) without GSH, c) without H_2O_2, d) with all components. B) Time-dependent absorbance changes of NADPH with different concentrations of GSH. C) Scavenging efficiency of superoxide radicals in different conditions: a) blank control without ultraviolet radiation, b) in the absence of nanocomposites after ultraviolet radiation, c) in the presence of hybrid nanocomposites after ultraviolet radiation. D) Percent inhibition of NBT oxidation with different concentrations of nanocomposites. E) Scavenging efficiency of hydroxy radical in different conditions. F) Percent inhibition of TA oxidation with different concentrations of nanocomposites.

apparent steady-state kinetic parameters were also measured with different concentrations of substrates (Figure S14). All the above results confirmed that our nanocomposites possessed excellent GPx-like activity to effectively remove excess H_2O_2.

In the human body, Mn, as one essential micronutrient, plays a significant role in life system. For example, Mn can be utilized as part of the manganese cofactor incorporated in several important enzymes.[14] Among them, one important enzyme is SOD.[14a,b] SOD can catalyze the disproportionation reaction of $O_2^{\bullet-}$,[6b] serving as one significant antioxidant enzyme in nearly all living cells. Previous work demonstrated that Mn-based materials possessed SOD-like property.[15] Therefore, in our system, V_2O_5@pDA@MnO_2 nanocomposites were used to mimic SOD (Figure S15). To verify our hypothesis, the SOD-like property of nanocomposites was studied.[16] In the presence of riboflavin, methionine and NBT, a strong fluorescence signal was obtained after UV irradiating, demonstrating the high level of superoxide (Figure 2C). Once the nanocomposites were present, the signal decreased dramatically, which was consistent with our hypothesis. We also compared the catalytic activities of different components. Figure S16 indicated our V_2O_5@pDA@MnO_2 nanocomposites showed comparable catalytic activity with MnO_2 nanomaterials. Figure S17 indicated the scavenging capacity enhanced with the increasing of nanocomposite concentration. In the presence of 15 $\mu g\,mL^{-1}$ nanocomposites, nearly 70% superoxides were removed (Figure 2D). These results further confirmed our hybrid system possessed excellent superoxide radical removal capacity.

Studies have demonstrated that MnO_2 nanomaterials can also possess CAT-like ability to catalyze the decomposition of H_2O_2 (Figure S18).[7a,8a] Herein, MnO_2 components were also used to eliminate harmful H_2O_2 and the CAT-mimic property of our nanocomposites was investigated.[17] With the assistance of nanocomposites, OH radical could be efficiently removed (Figure 2E). Furthermore, polydopamine could also serve as an efficient antioxidant to eliminate ROS. To verify this, the ROS removal capacities of V_2O_5 and V_2O_5@pDA nanomaterials were measured. Compared with V_2O_5 nanowire, a dramatically decrease of fluorescence signal was obtained in V_2O_5@pDA treated system, confirming polydopamine could efficiently eliminate reactive oxygen species. Compared with V_2O_5@pDA and MnO_2 nanomaterials, our V_2O_5@pDA@MnO_2 nanocomposites possessed higher OH radical scavenging ability, illustrating the synergetic antioxidative property of our system (Figures 2E and S19). Upon increasing the concentration of the nanocomposites, the scavenging activity enhanced gradually (Figure S20). In the presence of 80 $\mu g\,mL^{-1}$ nanocomposites, the scavenging rate could reach to around 85% (Figure 2F). We further investigated the durability of our nanocomposites and Figures S21 and S22 all confirmed the high stability and durability of our nanocomposites. We also investigated the effect of pH on biocatalytic capacities of our nanocomposites. In Figure S23, small changes of catalytic activities were obtained and under physiological pH conditions, our nanocomposites still remained high enzymatic capacities.

The successful verification of multienzyme-like properties of V_2O_5@pDA@MnO_2 nanocomposites inspired us to further explore their potential application for antioxidation in cellular microenvironment. Before that, the cytotoxicity of the nanocomposites was evaluated by methyl thiazolyl tetrazolium (MTT) assay. After incubating a series of concentrations of nanocomposites with HEK293T (human embryonic kidney) cells for 24 h, no obvious inhibiting effect on cell proliferation was observed (Figure S24). This result indicated that our system possessed good biocompatibility and was feasible for further biorelated usages.

We then investigated the intracellular antioxidant capacity of our nanocomposites. In order to measure the scavenging capacity of the nanocomplexes against intracellular ROS, the HEK293T cells were pretreated with the nanocomplexes and then treated with exogenously Rosup.[18] The intracellular ROS level could be monitored by using DCFH-DA as the fluorescence probe. As shown in Figure 3A, control experiment indicated when cells were incubated with the nanocomposites, negligible fluorescence signal was observed, demonstrating low cytotoxicity of our system. In contrast, a high fluorescence signal was observed when preincubated with Rosup. With the assistance of the nano-

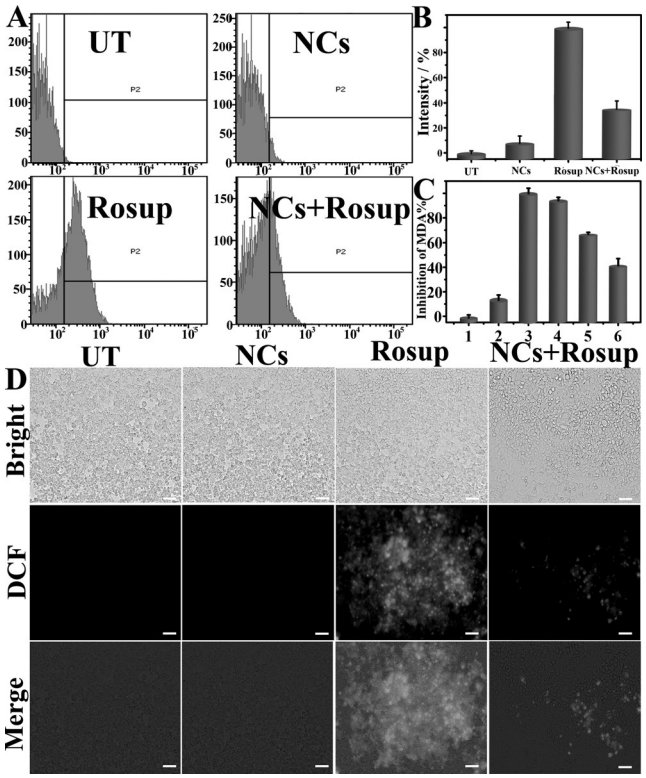

Figure 3. A) Flow cytometry analysis used to monitor the changes of intracellular ROS. B) Effect of the nanocomposites on ROS scavenging in HEK293T cells. C) Effect of the nanocomposites on lipid peroxidation: 1) control (untreated cells), 2) incubated with nanocomposites, 3) incubated with Rosup, 4–6) incubated with Rosup and different concentrations of nanocomposites. D) Fluorescence microscopy images of HEK293T cells with different treatments (scale bar, 50 μm).

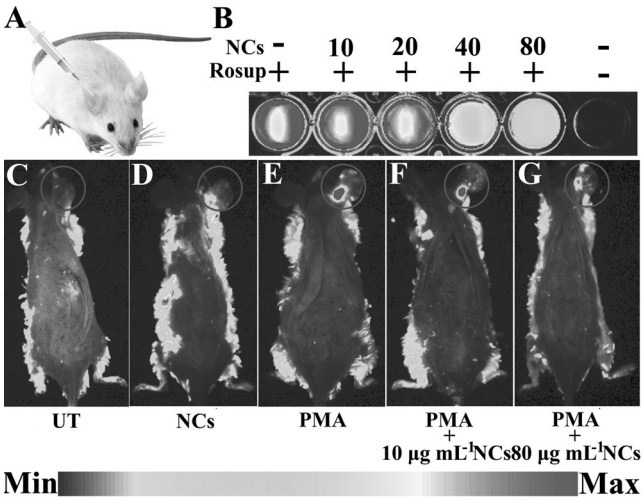

Figure 4. A) Scheme of the inflammation model. B) Luminescence images of various concentration of V_2O_5@pDA@MnO_2 hybrid nanocomposites (NCs) in the presence or absence of Rosup using in vivo imaging system. C) In vivo imaging of the effect of the nanocomposites on ROS scavenging in PMA-induced ear inflammation.

composites, the fluorescence intensity of Rosup treated cells decreased observably. Quantitative analysis illustrated that nearly 65% ROS could be removed efficiently (Figure 3B). Fluorescence microscopy images in Figure 3D further confirmed the antioxidant ability of our nanocomposites. As we had mentioned before, the overexpressed ROS in cells might cause detrimental influences.[3,4] Among them, one mainly damage was lipid peroxidation. The lipid peroxides in the cell could be quantified by measuring the final oxidative product in the lipid peroxidation reaction, malondialdehyde (MDA), with the thiobarbituric acid (TBA) assay.[6b] In Figure 3C, an increase of MDA was observed when cells were incubated with Rosup. With the assistance of different concentrations of the nanocomposites, the lipid peroxidation could be efficiently inhibited. All these above results illustrated our system could effectively suppress the generation of ROS and protect cells against oxidative stress.

We also constructed a simple inflammation model to explore the potential application (Figure 4A). In our work, we used the Kunming mouse as the model to investigate the body protective capacity of our nanocomposites. As displayed in Figure 4B, the luminescence of the in vivo imaging system was high in the presence of Rosup. When increasing the concentrations of the nanocomposites, the luminescence decreased gradually, revealing an enhancement of ROS removal efficiency. To generate endogenous ROS, we induced acute local inflammation in the ear by topical application of phorbol 12-myristate 13-acetate (PMA).[19] After the injection of PMA for 6 h, in vivo animal model imaging was recorded (Figure 4C–G). To study the ROS removal capability of our nanocomposites against inflammation, the ears were further treated with the nanocomposites. As demonstrated in Figure 4D, no obvious fluorescence was observed when only treated with the nanocomposites. In contrast, a strong luminescent signal was monitored in the PMA-treated ear (Figure 4E). With the assistance of the nanocomposites, the fluorescence intensity of the PMA-treated ear decreased. Compared with V_2O_5 or MnO_2 nanomaterials, our V_2O_5@pDA@MnO_2 nanocomposites presented enhanced ROS scavenging capacity (Figure S25). Upon increasing the concentrations of V_2O_5@pDA@MnO_2 nanocomposites, an enhancement of ROS scavenging capacity was obtained (Figure 4G). The above results indicated our system possessed excellent reactive oxygen species removal capacity in the mouse model and might have potential application in inflammation therapy.

In conclusion, we presented the first example of fabricating a novel multi-nanozyme cooperative platform to mimic intracellular antioxidant enzyme-based defense system. The distinctive advantage of our multi-nanozyme-based system was through self-assembling, the obtained V_2O_5@pDA@MnO_2 nanocomposite could serve as one multi-nanozyme model to mimic intracellular antioxidant defense procedure in which SOD, CAT, GPx, etc. coparticipate. In addition to the antioxidative activities of nanozymes, by assembling with dopamine, the nanocomposites provided synergistic antioxidative effect. Both in vitro and in vivo experiments demonstrated that our nanocomposites exhibited excellent intracellular reactive oxygen species removal ability to protect cell components against oxidative stress, showing its potential application in inflammation

therapy. Combined together, we expected that this work might help us further understand the reaction mechanism of the intracellular antioxidant enzyme-based defense system and would be highly beneficial in development of novel nanozyme-based cooperative system in future biochemical, nanomechanical and medicinal applications.

Acknowledgements

Financial support was provided by National Basic Research Program of China (Grants 2012CB720602) and the National Natural Science Foundation of China (Grants 21210002, 21431007, 21403209, 21533008).

Keywords: antioxidant defense system · nanozymes · oxidative stress · reactive oxygen species · self-assembly

How to cite: *Angew. Chem. Int. Ed.* **2016**, *55*, 6646–6650
Angew. Chem. **2016**, *128*, 6758–6762

[1] a) T. Wirth, *Angew. Chem. Int. Ed.* **2015**, *54*, 10074–10076; *Angew. Chem.* **2015**, *127*, 10212–10214; b) C. C. Winterbourn, *Nat. Chem. Biol.* **2008**, *4*, 278–286.

[2] a) T. S. Gechev, F. V. Breusegem, J. M. Stone, I. Denev, C. Laloi, *BioEssays* **2006**, *28*, 1091–1101; b) M. Schieber, N. S. Chandel, *Curr. Biol.* **2014**, *24*, R453–R462.

[3] a) T. Finkel, *J. Biol. Chem.* **2012**, *287*, 4434–4440; b) H. Sies, *Angew. Chem. Int. Ed. Engl.* **1986**, *25*, 1058–1071; *Angew. Chem.* **1986**, *98*, 1061–1075; c) I. D. Donne, G. Aldini, M. Carini, R. Colombo, R. Rossi, A. Milzani, *J. Cell. Mol. Med.* **2006**, *10*, 389–406.

[4] a) L. W. Oberley, G. R. Bueftner, *Cancer Res.* **1979**, *39*, 1141–1149; b) R. A. Cairns, I. S. Harris, T. W. Mak, *Nat. Rev. Cancer* **2011**, *11*, 85–95; c) F. Giacco, M. Brownlee, *Circ. Res.* **2010**, *107*, 579–591; d) S. Reuter, S. C. Gupta, M. M. Chaturvedi, B. B. Aggarwal, *Free Radical Biol. Med.* **2010**, *49*, 1603–1616.

[5] a) L. A. Sena, N. S. Chandel, *Mol. Cell* **2012**, *48*, 158–167; b) S. Hussain, W. Slikker, Jr., S. F. Ali, *Int. J. Dev. Neurosci.* **1995**, *13*, 811–817; c) C. Michiels, M. Raes, O. Toussaint, J. Remacle, *Free Radical Biol. Med.* **1994**, *17*, 235–248.

[6] a) D. Bhowmick, S. Srivastava, P. D'Silva, G. Mugesh, *Angew. Chem. Int. Ed.* **2015**, *54*, 8449–8453; *Angew. Chem.* **2015**, *127*, 8569–8573; b) H. C. Sun, L. Miao, J. X. Li, S. Fu, G. An, C. Y. Si, Z. Y. Dong, Q. Luo, S. J. Yu, J. Y. Xu, J. Q. Liu, *ACS Nano* **2015**, *9*, 5461–5469; c) S. J. Yu, Y. Z. Yin, J. Y. Zhu, X. Huang, Q. Luo, J. Y. Xu, J. C. Shen, J. Q. Liu, *Soft Matter* **2010**, *6*, 5342–5350.

[7] a) X. Liu, Q. Wang, H. H. Zhao, L. C. Zhang, Y. Y. Su, Y. Lv, *Analyst* **2012**, *137*, 4552–4558; b) Y. Y. Li, X. He, J. J. Yin, Y. H. Ma, P. Zhang, J. Y. Li, Y. Y. Ding, J. Zhang, Y. L. Zhao, Z. F. Chai, Z. Y. Zhang, *Angew. Chem. Int. Ed.* **2015**, *54*, 1832–1835; *Angew. Chem.* **2015**, *127*, 1852–1855.

[8] a) P. Prasad, C. R. Gordijo, A. Z. Abbasi, A. Maeda, A. Ip, A. M. Rauth, R. S. DaCosta, X. Y. Wu, *ACS Nano* **2014**, *8*, 3202–3212; b) C. Xu, X. G. Qu, *NPG Asia Mater.* **2014**, *6*, e90; DOI: 10.1038/am.2013.88; c) A. Watanabe, M. Kajita, J. Kim, A. Kanayama, K. Takahashi, T. Mashino, Y. Miyamoto, *Nanotechnology* **2009**, *20*, 455105; d) A. A. Vernekar, D. Sinha, S. Srivastava, P. U. Paramasivam, P. D'Silva, G. Mugesh, *Nat. Commun.* **2014**, *5*, 5301–5313.

[9] R. André, F. Natálio, M. Humanes, J. Leppin, K. Heinze, R. Wever, H. C. Schröder, W. E. G. Müller, W. Tremel, *Adv. Funct. Mater.* **2011**, *21*, 501–509.

[10] K. G. Qu, P. Shi, J. S. Ren, X. G. Qu, *Chem. Eur. J.* **2014**, *20*, 7501–7506.

[11] a) H. Lee, S. M. Dellatore, W. M. Miller, P. B. Messersmith, *Science* **2007**, *318*, 426–430; b) Q. L. Fan, K. Cheng, X. Hu, X. W. Ma, R. P. Zhang, M. Yang, X. M. Lu, L. Xing, W. Huang, S. S. Gambhir, Z. Cheng, *J. Am. Chem. Soc.* **2014**, *136*, 15185–15194.

[12] H. Jiang, L. P. Yang, C. Z. Li, C. Y. Yan, P. S. Lee, J. Ma, *Energy Environ. Sci.* **2011**, *4*, 1813–1819.

[13] K. P. Bhabak, G. Mugesh, *Chem. Eur. J.* **2007**, *13*, 4594–4601.

[14] a) C. E. Valdez, Q. A. Smith, M. R. Nechay, A. N. Alexandrova, *Acc. Chem. Res.* **2014**, *47*, 3110–3117; b) M. E. Martin, B. R. Byers, M. O. J. Olson, M. L. Salin, J. E. L. Arceneaux, C. Tolbert, *J. Biol. Chem.* **1986**, *261*, 9361–9367; c) K. Bhardwaj, L. Guarino, C. C. Kao, *J. Virol.* **2004**, *78*, 12218–12224.

[15] S. Miriyala, I. Spasojevic, A. Tovmasyan, D. Salvemini, Z. Vujaskovic, D. St. Clair, I. B. Haberle, *Biochim. Biophys. Acta Mol. Basis Dis.* **2012**, *1822*, 794–814.

[16] M. Li, S. E. Howson, K. Dong, N. Gao, J. S. Ren, P. Scott, X. G. Qu, *J. Am. Chem. Soc.* **2014**, *136*, 11655–11663.

[17] Z. J. Zhang, M. Li, J. S. Ren, X. G. Qu, *Small* **2015**, *11*, 1258–1264.

[18] M. Xie, N. N. Lu, S. B. Cheng, X. Y. Wang, M. Wang, S. Guo, C. Y. Wen, J. Hu, D. W. Pang, W. H. Huang, *Anal. Chem.* **2014**, *86*, 4618–4626.

[19] a) A. Kielland, T. Blom, K. S. Nandakumar, R. Holmdahl, R. Blomhoff, H. Carlsen, *Free Radical Biol. Med.* **2009**, *47*, 760–766; b) G. Pozsgai, K. Sándor, A. Perkecz, J. Szolcsányi, Z. Helyes, S. D. Brain, E. Pintér, *Inflammation Res.* **2007**, *56*, 459–467.

Received: January 26, 2016
Published online: April 21, 2016

